Analysis and Design of Energy Storage for Current-Source 1-ph Grid-Connected PV Inverters

G. Ertasgin, D.M. Whaley, N. Ertugrul and W.L. Soong

School of Electrical and Electronic Engineering

University of Adelaide, Adelaide, Australia

gurhan@eleceng.adelaide.edu.au

Abstract- **This paper examines the analysis and design of a DC link inductor for a current source 1-ph grid-connected photovoltaic (PV) inverter. Firstly the effect of voltage or current ripple on the PV array average output power is examined using a normalized PV output characteristic. Secondly the design of the inductor and in particular the trade-off between the PV array output power loss and the inductor copper loss are discussed. An inductor was built and a comparison of the calculated and measured loss breakdown is presented.**

I. INTRODUCTION

The research interest in renewable energy sources is increasing due to the world's increasing energy consumption, global warming and pollution. Grid-connected photovoltaic (PV) inverters have become more economically viable owing to advances in PV cell and semiconductor technology.

Single-phase small-scale grid-connected inverters (GCI) have a 100 Hz instantaneous power output variation which causes fluctuations in the PV cell output power. All single-phase GCIs employ an energy storage element to keep the PV cell output power relatively constant and hence maximize the average PV output power. The energy storage element is a DC link capacitor for a voltage-source inverter (VSI) and a DC link inductor for a current-source inverter (CSI). It is important to keep the required energy storage as small as possible to reduce its size and cost.

A. Energy Storage in Single-Phase Current-Source GCI

Current-source GCIs are designed to feed sinusoidal current into the grid at unity power-factor. Fig. 1 shows the PV cell ripple current, the instantaneous inverter input voltage, input power and the output power. The instantaneous output power of the inverter has a frequency of 100 Hz and a magnitude of twice the average output power. Since the inverter has no internal storage element the instantaneous inverter input power and output power must be the same assuming an ideal (lossless) inverter. Therefore in order to reduce the instantaneous power fluctuation seen by the PV array a DC link inductor is used. The average power generated by the PV array (dashed line) is the same as the average power fed into the grid.
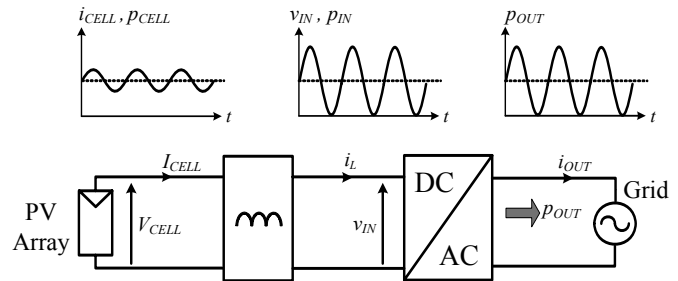

Fig. 1. Single-phase current-source GCI showing the PV array, the DC link inductor, inverter, power grid and relevant waveforms.

The stored energy in the inductor depends on the current. The power fluctuations change the stored energy in the inductor. Therefore the inductor current and hence the PV array current vary. This variation results in a reduction in the average output power of the PV array although the average PV current may still be the current at the maximum power point (I_0) as shown in Fig. 2. This is because the maximum power only occurs when the current is at I_0 so any variation causes a reduction in the PV array output power.
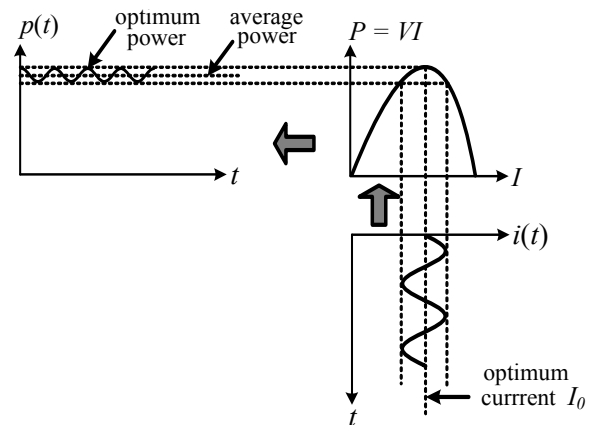

Fig. 2. PV array output current variations cause a reduction in the average PV array output power, for a CSI.

The PV array power reduction due to output power fluctuations has been taken into account when designing inverters as reported in the literature. Kjaer examined the effect of voltage ripple on a VSI for both standard silicon and

cadmium-telluride (CdTe) PV arrays [1]. He assumed the sinusoidal voltage ripple was centered around the optimum voltage. Kjaer modelled the PV array power voltage curve around the PV cell's maximum power point (MPP) using a second-order Taylor series to find an acceptable voltage ripple for average power reductions from 0.1% to 2%. The relationship between the capacitor size and the voltage ripple was also analysed.

In [2], Casadei et al. used the voltage ripple for MPP tracking for a VSI. The voltage ripple is a function of average output power P_0, grid angular frequency ω and the DC link capacitance C_{DC} :

$$\frac{P_0}{\omega} = C_{DC}(V_{dcMAX}^2 - V_{dcMIN}^2) \qquad (1)$$

Some preliminary work has been done by the authors to examine the effect of current ripple in a CSI using a similar expression to equation (1) [3].

The aim of this paper is to examine the design of the DC link inductor for a single phase 150 W current source GCI. The paper includes the effect of the inductor value and the PV array power output loss caused by the power fluctuations, and test results on the inductor losses.

II. Effect of Ripple on Average PV Array Output Power

This section analyses the behavior of the PV array average output power as a function of output current and voltage ripple. Analysis of the PV array I-V locus shows that the basic shape is not significantly affected by irradiance and temperature variations. The result is used for average output power loss calculation for a given current or voltage ripple.

A. PV Array Model

PV arrays consist of series or parallel PV modules. For modeling the PV array, the simple diode model has been used to show the relationship between the PV array voltage and current [4]:

$$I = I_{SC}(1 - e^{(V + IR_S - V_{OC})/(nV_T N_S)}) \qquad (2)$$

where, I_{SC} is the short circuit current, R_S is the total series resistance, V_{OC} is the open-circuit voltage, n is the diode ideality factor, V_T is the thermal voltage and N_S is the number of series connected cells.

B. PV Array Prediction Results

The array consists of two series-connected 80 W PV modules (BP380J) which produce about 150 W output power [5]. Table 1 lists the parameters of the PV module. These parameters are used in equation (2) for simulations including the effect of cell temperature and solar irradiation variations.

TABLE I
SPECIFICATIONS OF THE 80 W BP SOLAR BP380J

Parameter	Value
Rated Maximum Power (P_0)	80 W
Voltage at P_0 (V_0)	17.6 V
Current at P_0 (I_0)	4.55 A
Short Circuit Current (I_{SC})	4.8 A
Open Circuit Voltage (V_{OC})	22.1 V
Temperature Coefficient of I_{SC} (α)	(0.065±0.015)% / °C
Temperature Coefficient of V_{OC} (β)	-(80±10)mV/ °C
Resistance for module (R_S)	0.034 Ω

The effect of solar irradiance variations is investigated in Fig 3. This shows the current-voltage and power-voltage loci for irradiances of G = 250-1000W/m^2, at a cell temperature of 25°C.
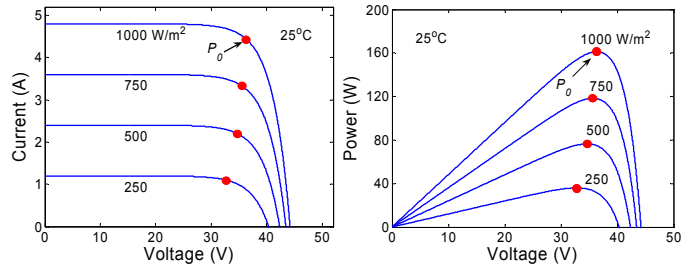

Fig. 3. Calculated effect of solar irradiance variation on the current-voltage (left) and power-voltage (right) loci, for the standard cell temperature of 25°C. The dots represent the maximum power point.
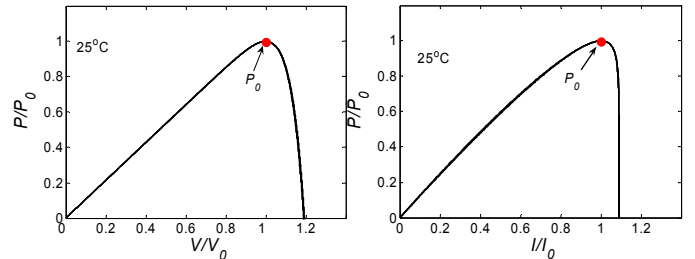

Fig. 4 . Normalised calculated power-voltage (left), and power-current (right) loci, for varying solar irradiance at 25°C.

Fig. 4 (left) shows the power-voltage curves which are the same as Fig. 3 (right), after individually normalizing each curve so that the MPP voltage V_0 and power P_0 are 1 pu. The current-voltage loci given in Fig. 3 (left) can also be used to plot the power-current loci. These power-current loci can be individually normalised to give the MPP current I_0 and power P_0 as 1 pu and the result is shown in Fig. 4 (right).

The effect of cell temperature variation can be seen in Fig. 5, for a temperature range of 0 to 75°C, and a solar irradiance of 1000W/m^2. The normalised P-V and P-I loci, for the same temperature range are shown in Fig. 6.

It is important to note that the normalised shape of the power-voltage and power-current curves are largely unaffected by the temperature and the irradiation variations. The following calculations were thus done using the normalised curves under standard test conditions (1000 W/m^2 and 25 °C).
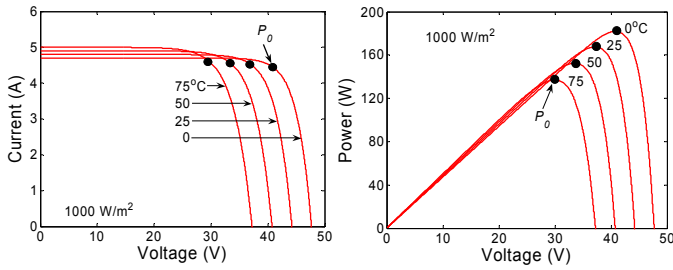
1230

Fig. 5. Calculated effect of temperature variation on the current-voltage (left) and power-voltage (right) loci, for the standard irradiance of 1000W/m².
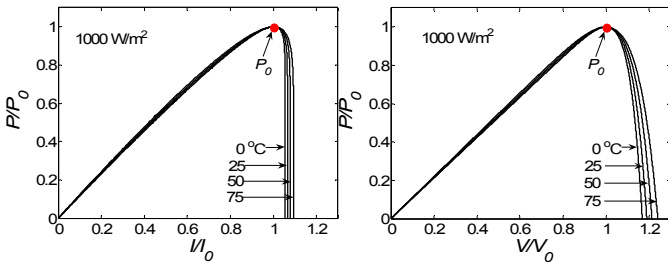

Fig. 6. Normalised power-current (left), and power-voltage (right) loci, for the array temperature variations.

C. Average Output Power Reduction Due to Ripple

This section analyses the power loss caused by ripple, using the normalized curves under standard test conditions. Fig. 7 provides two different approaches for defining the peak to peak ripple (ΔI). Fig. 7 (left) shows the definition used by Kjaer [1] where the ripple is "centered" on the MPP current I_0. An alternative definition proposed in this paper is the "balanced" approach shown in Fig. 7 (right). This definition makes the output power equal at the current extremes. The centered definition gives a reasonable approximation at small values of ripple (see Fig. 8), however the balanced definition provides greater output power and so more accurately represents the operating point that is tracked by the MPP algorithm.
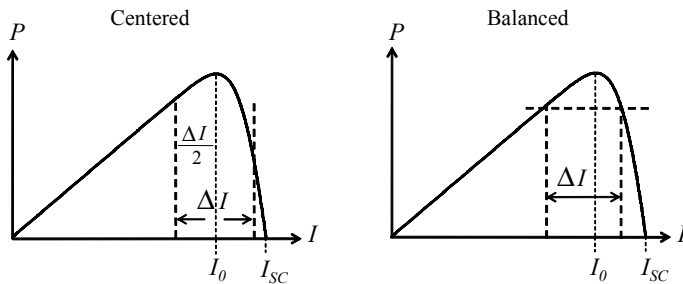

Fig. 7. Definition of centred (left) and balanced assumptions for ΔI (right)

Fig. 8 compares the average power reduction due to voltage or current ripple for both the centered and the balanced method. This figure is based on the normalised power-current and power-voltage curves under standard conditions, and the two ripple definitions. It assumes a sinusoidally time-varying voltage or current ripple (see Fig. 2) and then calculates the resultant instantaneous output power waveform, and hence the average power reduction.

The curves for the balanced voltage ripple and balanced current ripple are nearly identical. The centered ripple definition gives higher values of power reduction, particularly for the centered current ripple case at higher ripple magnitudes.

Both balanced and centered definitions give similar results for small values of ripple but they diverge as the ripple increases; e.g. a 12% current ripple yields a 2.1% power reduction using the centered definition, however the balanced definition yields only 1.3%.

For comparison purposes, the calculated results from [1] based on the centered voltage-ripple definition are also shown in Fig. 8 as circles. This used a second-order Taylor series approximation for the PV array power versus voltage characteristic. It shows a good correspondence with the centered voltage ripple result at low values of ripple, but diverges significantly at higher ripple values due to the Taylor series approximation to the power-voltage curve.
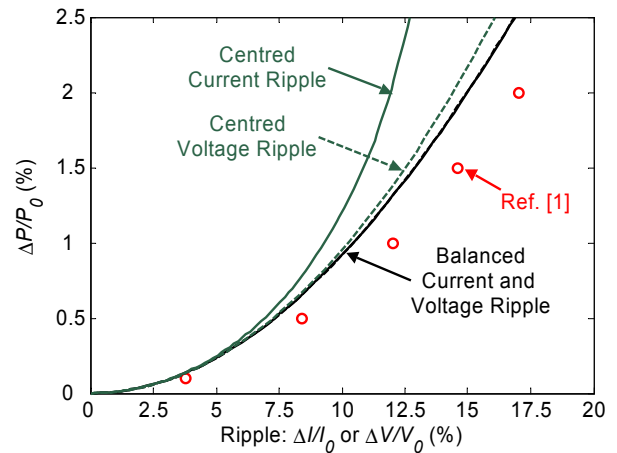

Fig. 8. Average power reduction versus voltage ripple (dashed lines) and current ripple (solid lines) using both centred and balanced ripple definitions. The centred voltage ripple results from [1] are shown as circles.

III. CURRENT AND VOLTAGE RIPPLE AS A FUNCTION OF ENERGY STORAGE

Fig. 1 showed a single-stage current-source inverter, along with the inverter input (inductor) current, $i_L(t)$, and the instantaneous output power, $p_{OUT}(t)$. The output power shows a 100 Hz variation. It will initially be assumed that the inductor current $i_L(t)$ is essentially constant. The inverter input voltage $v_{IN}(t)$ is given by :

$$v_{IN}(t) = \frac{p_{OUT}(t)}{i_L(t)} \qquad (3)$$

As the inductor acts as a short circuit to DC, it can also be assumed that v_{CELL} is essential constant and has a value that is equal to the average value of $v_{IN}(t)$. If it is initially assumed that both $i_L(t)$ and V_{CELL} are constant then the output power of the PV cells is constant though the instantaneous input power of the inverter is time-varying. This implies the DC link inductor must provide the required energy storage by absorbing or releasing the difference in power between what

the PV cell provides and what the inverter requires. The stored energy in the inductor has a ripple of ΔE and varies as a function of current, and so the inductor current $i_L(t)$ must vary with time. Considering the voltages, it can be seen that the inductor voltage is equal to the difference between the PV cell voltage V_{CELL} and the inverter input voltage v_{IN}, and is hence a sine wave with zero mean. The inductor current is thus a cosine waveform with an offset equal to the mean PV cell current. Based on this, it is possible to show an approximate relationship between the size of the DC link inductor and the current ripple.

The average energy E_0 stored in the DC inductor L is given by :

$$E_0 = \tfrac{1}{2} L I_0^2 \qquad (4)$$

The inductor energy ripple ΔE is :

$$\Delta E = \int_0^{T/2} V_0 I_0 \sin(\omega t)\,dt = \frac{1}{\pi} V_0 I_0 T = \frac{P_0}{\omega} \qquad (5)$$

where T is the period of the instantaneous power waveform, P_0 is the average inverter output power and ω is the angular frequency of the grid voltage. For small values of ripple, it can be shown that the current ripple ΔI can be related to the energy ripple ΔE by:

$$\Delta E = LI_0\Delta I \qquad (6)$$

This can be re-arranged to show that:

$$\frac{\Delta i}{I_0} = \frac{\Delta E}{2E_0} = \frac{P_0}{2\omega E_0} \qquad (7)$$

A similar calculation could be performed for PV VSI inverters with a large parallel DC link capacitor to obtain:

$$\frac{\Delta v}{V_0} = \frac{\Delta E}{2E_0} = \frac{P_0}{2\omega E_0} \qquad (8)$$

Thus a simple relationship can be seen between the current (and voltage) ripple, the output power and the stored energy E_0.

TABLE 2
EXISTING VOLTAGE SOURCE PV GCI DESIGN EXAMPLES BASED ON
BALANCED METHOD

Ref	Grid Freq. (Hz)	P_0 (W)	Capacitor (mF)	V_0 (V)	E_0 (J)	ΔV (V)	$\Delta V/V_0$	$\Delta P/P_0$
[6]	50	80	6.8	48.7	8.1	1.35	1.6%	0.04%
[7]	60	600	3	137	30	3.87	2.8%	0.05%

Table 2 examines two existing VSI grid-connected inverter designs [6-7] and provides data on the grid frequency, output power, DC link capacitor and MPP output voltage. Equation (8) is applied to the data provided and hence the voltage ripple ΔV and the average PV power reduction can be estimated

(using the balanced ripple definition). Both designs yield <0.1% average power reduction.

IV. INDUCTOR DESIGN FOR 150 W CSI

The design of the inductor for a PV grid-connected CSI has an important trade-off with regards to its sizing: the larger the energy storage, the lower the current ripple and hence PV average power loss; but the larger the inductor's size, cost and power losses (P_{CU}). Fig. 9 (left) illustrates this trade-off for a 150 W inverter using a particular inductor magnetic design (192 mH). Fig. 9 (right) shows another trade-off regarding how the copper losses decrease as the wire diameter increases; however the relative copper costs (volume), and packing factor increases.
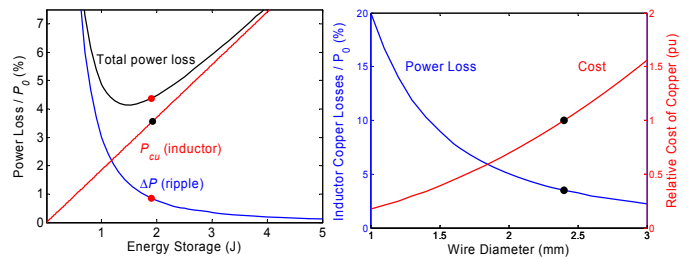

Fig. 9. Inductor design trade-off graphs, showing (left) total power loss vs. energy storage, and (right), the copper power loss and relative cost vs. wire diameter. The circles represent the values of the 150 W 192 mH inductor.

The 150 W inverter is shown in Fig. 10; it uses a similar topology to Fig. 1 with two series-connected BP380J PV modules. The PV cells are covered from the light and connected to a constant-current power supply to simulate the PV array output using the dark-IV method [3].
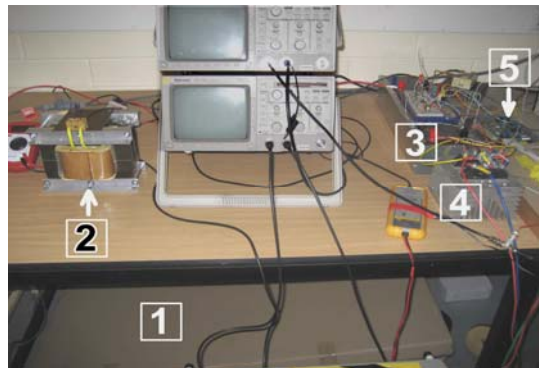

Fig. 10. Grid-connected CSI set-up showing light covered PV modules (1), the 192 mH inductor (2), current wave-shaper (3), thyristor based inverter (4) and microcontroller (5).

Two inductors were designed and built for the 150 W CSI inverter, one with a stored energy of approximately 1 J (actually 1.15 J, 112 mH) and one with a stored energy of approximately 2 J (actually 1.96 J, 192 mH). The inductors were both constrained to have copper losses which were of the order of 5 W. Their characteristics are listed in Table 3. Both

1232

the 192 mH inductor (see Fig 10) and the 112 mH inductor are designed for the rated PV cell current (I_0) that corresponds to peak power (P_0). The calculated peak to peak current ripple ($\Delta I/I_0$) is around 13% for the large inductor.

TABLE 3
PARAMETERS OF THE TWO INDUCTORS FOR THE CSI PV INVERTER

Parameter	Inductor 1	Inductor 2
Rated maximum input power (P_0)	150 W	150 W
Input current for P_0 (I_0)	4.5 A	4.5 A
Input voltage (V_O)	35 V	35 V
Inductance (L)	112 mH	192 mH
Stored energy	1.15 J	1.96 J
Diameter of the copper wire	2.4 mm	2.4 mm
Number of turns (N)	249	200
Resistance at 40°C (R_{CU})	0.25 Ω	0.324 Ω
Power losses in the inductor (P_{CU})	5.0 W	6.7 W
Current ripple (peak-to-peak)	21.3 %	12.8 %
Peak flux density (B)	1.5 T	1 T
Copper winding packing factor	0.46	0.37
Volume	0.00052 m^3	0.0021 m^3
Mass	5.5 kg	15.5 kg

V. EXPERIMENTAL RESULTS

Fig. 11 shows the measured inductance vs. AC rms current. Two measurement methods were used, firstly instantaneous flux-linkage λ based on integrating $v(t) - i(t)R$, and secondly using AC reactance. Both methods gave similar results.
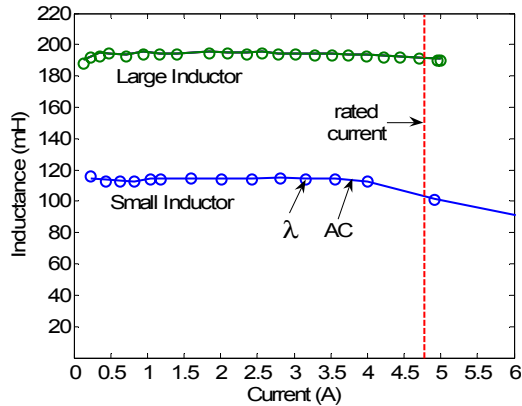

Fig. 11. Measured inductance of the two 150 W DC link inductors

The 150 W CSI design has a higher value of P_0/E_0 than the VSIs shown in Table 2. This causes the PV cell current ripple and hence average PV array power loss to be significantly larger for the CSI. The ripple associated power loss can be reduced by increasing the storage energy of the inductor at the expense of increased inductor losses (see Fig. 9 (left)).

Up to this point the inductor losses are assumed to be resistive (copper losses), however the inductor core also has iron losses which include hysteresis and eddy-current losses. Fig. 12 shows the measured larger (192 mH) inductor iron losses at 50 Hz, as a function of both current and voltage. Presuming that half of the iron loss is hysteresis and the other half is eddy-current, the losses with the 100 Hz fluctuation

was consistently estimated at about 0.08 W from both the rated inductor current and voltage ripple (see Table 4) at MPP.
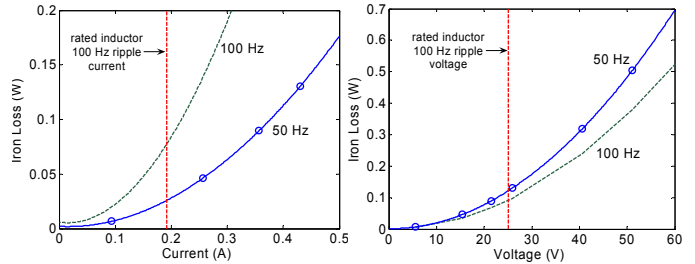

Fig. 12 . Iron loss vs. coil current (left), iron loss vs. voltage (right) for the 192 mH inductor. Measured 50 Hz test points (circles) and estimated 100 Hz loss (dashed line).

Fig. 13 shows the simulated and measured inverter input and output currents, that correspond to the PV array's MPP. The current ripple is about 13.4% which matches with the calculated Table 3 result. The output current waveform shows significant higher order harmonics, these are associated with resonances in the low-pass output filter which requires further optimization.
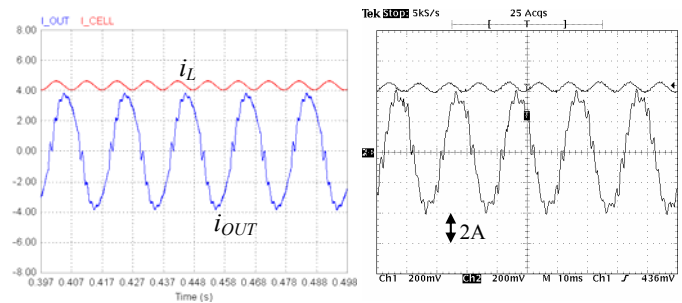

Fig. 13 . The simulated (left) and measured (right) waveforms for the inductor ripple current (i_L) and the CSI output current (i_{OUT}).

Fig.14 (left) shows the measured PV cell voltage, current and power waveforms. Fig. 14 (right) shows the measured inverter input voltage, current and power waveforms. The indicated power variations in Fig. 2 can also be seen in Fig 14.
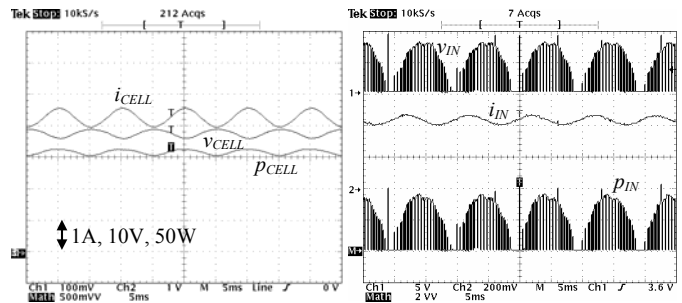

Fig. 14. The measured PV cell current, voltage and power waveforms (left), the measured inverter input voltage, current and power waveforms respectively (right).

Fig. 15 shows the measured PV cell power vs. modulation index for the 150 W grid-connected CSI showing the maximum power point.
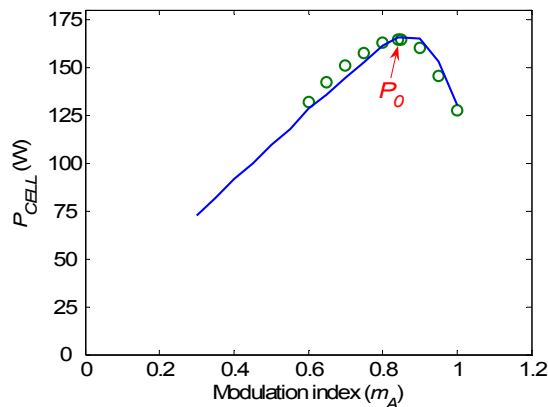
Fig. 15. The PV cell output power vs. modulation index, simulation results (line) and experimental results (circles).

Table 4 provides the simulation and test results for the 150 W current-source GCI describing the PV cell ripple and the inductor losses.

TABLE 4
150 W GCI INDUCTOR TEST RESULTS

	192 mH Inductor	
	Calculated	Tests
Maximum Power Point		
V_{CELL}	38.3 V	36.97 V
I_{CELL}	4.33 A	4.39 A
P_{CELL}	166.6 W	162.9 W
PV cell ripple analysis		
v_{CELL} (p-p)	12.7 %	7.6 %
i_{CELL} (p-p)	13.0 %	13.4 %
p_{CELL} (p-p)	2.65 %	6.10 %
p_{LOSS} (ripple)	1.33 %	3.10 %
Total PV power reduction	2.22 W	5.00 W
Inductor losses:		
DC copper loss	6.07 W	5.86 W
100 Hz copper + iron loss	0.09 W	0.15 W
PWM loss	-	0.10 W
Total inductor loss	6.16 W	6.11 W
PV cell power reduction and inductor losses	8.38 W	11.11 W

The measured PV array current ripple (13.4%) shows a good correspondence with the simulated results (13.0%) however the measured voltage ripple was much less than the calculated value. This is likely to be due to bandwidth issues associated with the constant-current power supply used for the dark-IV arrangement. This power supply has output capacitance which reduces its output impedance at 100 Hz. When the constant-current power supply was connected directly to the PV array, the measured voltage ripple was only about 30% of the simulated value. A 12 Ω resistor was then inserted between the power supply and the PV array in order to increase its high-frequency output impedance which increased the measured PV array voltage ripple to 60% of the simulated value. This confirmed the output impedance issue. Unfortunately it was not possible to use higher value series resistances due to output voltage constraints of the power supply. This effect also caused the PV array output power reduction to have significant error as it was assumed that the power reduction was equal to half the peak to peak ripple in the instantaneous PV array power.

The inductor loss breakdown was done by using power analyzer (Voltech PM3000A). The 100 Hz copper and iron losses have been acquired by using the power analyzer's harmonic analysis of the voltage and current waveforms. The PWM losses were determined as the difference between the total measured losses and the sum of the measured DC and 100 Hz losses.

VI. CONCLUSIONS

This paper examined the analysis and design of the DC link inductor for a single-phase photovoltaic grid-connected inverter. The key results are as follows:

- the shape of the normalised PV array power-voltage and power-current curves are not sensitive to irradiance or temperature variations;
- the definition of "balanced" current (or voltage) ripple based on equal power reduction at the extreme values gives more realistic estimates of PV output power reduction than assuming the ripple is centered on the optimum value;
- using the balanced definition, the average power reduction versus ripple magnitude is very similar for both voltage and current ripple;
- the voltage and current ripple is directly related to the ratio of output power to stored energy in the capacitor or inductor;
- there is a trade-off between the inductor size and the PV average power reduction;
- a 100 mH and a 200 mH DC link inductor was designed and built for a 150 W inverter;
- the inductor losses are largely resistive due to the large DC current component;
- there was a good correspondence between both the measured and calculated PV array output current ripple and the inductor losses.

The above results give a basis to select the required amount of energy storage to meet a given amount of acceptable average power loss.

REFERENCES

[1] S.B. Kjaer, "Design and control of an inverter for photovoltaic applications," Ph.D. dissertation, Inst. Energy Technol., Aalborg University, Aalborg East, Denmark, 2004/2005.
[2] D. Casadei, G. Grandi, and C. Rossi, "Single-Phase Single-Stage Photovoltaic Generation System Based on a Ripple Correlation Control Maximum Power Point Tracking," *IEEE Transaction on Energy Conversion*, vol. 21, pp. 562-568, 2006.
[3] G. Ertasgin, D.M. Whaley, N. Ertugrul, and W.L. Soong, "A Current-Source Grid-Connected Converter Topology for Photovoltaic Systems", *Proceeding of AUPEC 2006*, Melbourne, Australia, Dec. 2006.
[4] R.L. Castaner and S. Silvestre, *Modelling Photovoltaic Systems using PSpice*, Wiley, Chichester, U.K., 2002.
[5] BP380 solar module data sheet http://www.bp.com/sectiongeneric article.do?categoryId=9012977&contentId=7024400 [accessed 26 Nov. 2007]
[6] Y. Chen and K.M. Smedley, "A Cost-Effective Single-Stage Inverter with Maximum Power Point Tracking", *IEEE Transactions on Power Electronics*, pp. 1289-1294, Vol. 19, Sept. 2004
[7] F. Scapino and F. Spertino, "Circuit Simulation of Photovoltaic Systems for Optimum Interface between PV Generator and Grid", *IEEE IECON 02 Conference*, Vol. 2, Nov. 2002.